First-principles calculation of the electronic, dielectric, and dynamical properties of CaF_2

Matthieu Verstraete* and Xavier Gonze
Unité de Physico-Chimie et de Physique des Matériaux (PCPM), Université Catholique de Louvain, 1 Croix du Sud, B-1348 Louvain-la-Neuve, Belgium

(Received 27 May 2003; revised manuscript received 2 September 2003; published 26 November 2003)

Calcium fluoride is a prototypical very large band-gap material, with applications in far-ultraviolet optics. We study the electronic, dielectric, and vibrational properties of CaF_2 from first principles, using density-functional theory. The phonon band structure is well reproduced with standard pseudopotentials, except for one optical T_{1u} mode near Γ and X. However, the calculated dielectric properties are very poor. Improving the quality of the dielectric constants of the crystal requires a pseudopotential for Ca with additional semicore electrons. We perform a detailed analysis of the static and dynamical charges, as well as the interatomic force constants.

DOI: 10.1103/PhysRevB.68.195123 PACS number(s): 77.22.−d, 63.20.−e, 78.20.−e

I. INTRODUCTION

Very large scale integration in microelectronics has been made possible by the development of photolithographic methods: a photosensitive resin is exposed using ultra-violet (UV) radiation passing through a mask. Semiconductor circuits can be mass-produced with typical feature sizes down to 0.13 μm as of 2003. The further reduction of transistor sizes is limited by the wavelength of the UV radiation. The use of shorter wavelength light, in particular, x rays might circumvent this problem. However, as the wavelength decreases, it becomes more and more difficult to make lenses to focus the radiation. For far-UV radiation lenses, the present material of choice is calcium fluoride, or fluorite, CaF_2. The search for better materials is however ongoing; one of the main problems of fluorite is birefringence, which appears for very short wavelengths,[1] despite the cubic symmetry.

Experimental characterizations abound for CaF_2, especially as a host lattice for heavy atoms in fluorescence studies (see, e.g., Ref. 2). The phonon spectrum was determined experimentally by Elcombe and Pryor[3] as early as 1970. The stress dependence of phonon modes was investigated in the early 1980s.[4,5] However, little theoretical work exists on CaF_2's crystalline structure and properties, despite the simple structure it adopts. The electronic band structure of CaF_2 was determined first by Albert *et al.*,[6] who added an empirical potential to correct the conduction-band structure, then by Heaton and Lin[7] with a pure self-consistent-field method. The optical properties have been studied more recently by Shirley and co-workers,[1,8] and in particular the intrinsic quality of the birefringence in CaF_2 at short wavelengths. On a side note, de Leeuw *et al.*[9] studied the effect of water on the surface of CaF_2, and determined some of its electronic properties. Finally, the zone-center phonons, elastic constants, and total energies were determined *ab initio* using different techniques [Hartree-Fock, density-functional theory (DFT)] very recently in several different approximations, by Mérawa and co-workers.[10] We are aware of on-going work (both experimental and theoretical) on phonons in CaF_2 and other fluorides by K. Schmalzl and co-workers.[11]

Given the widespread use of CaF_2, its technological importance, and the present drive beyond the limit of ''traditional'' photolithographic techniques, the theoretical characterization of fluorite is of general interest. We determine the electronic, dielectric, and vibrational properties of fluorite, including the full phonon and electron band structures and the interatomic force constants, through density-functional theory[12,13] methods. We use the ABINIT (Ref. 14) software package, which employs a plane-wave basis set, and implements density-functional perturbation theory (DFPT) for the determination of the linear response to atomic displacements and electric fields. CaF_2 is an ionic material, and we estimate the charge on each atom by two different methods. The rest of this article is organized as follows: the theoretical methods and the system are described in Sec. II. The resulting electronic and phononic band structures and related properties are presented in Sec. III. Our conclusions are presented in Sec. IV. Atomic units are used throughout, unless otherwise specified.

II. THEORETICAL METHOD

We employ a standard implementation of DFT theory, with the wave functions represented in a plane-wave basis set, and periodic boundary conditions.[14] A review of the method (and of the algorithms used for the convergence of the electronic density and atomic positions) can be found in Ref. 15. CaF_2 is a cubic compound with three atoms per primitive face-centered-cubic unit cell (Ref. 16 group IVa1) in the reduced positions Ca (0,0,0) and F $\pm$(1/4,1/4,1/4). The Broyden algorithm[17] is used to relax the lattice parameter.

The effect of the approximation to the exchange-correlation (XC) energy is considered, comparing the local-density approximation (LDA) (from Perdew and Wang,[18] parametrized with electron-gas data by Ceperley and Alder[19]) to the generalized gradient approximation (GGA) of Perdew *et al.*[20]

Norm-conserving pseudopotentials of the Troullier-Martins[21] (TM) type are chosen to describe the interaction between the valence electrons and the nuclei and core electrons. A nonlinear-core-correction (NLCC) (Ref. 22) simulates the nonlinear XC effects of the core electrons, which overlap the valence s states substantially in calcium. The

plane-wave kinetic-energy cutoff for the basis set is 50 Ha with the pseudopotentials generated, for which the lattice parameter is converged to 0.04%. To limit the computational time, for phonons we use a slightly lower cutoff of 40 Ha: the lattice parameter is only converged to within 1% but the phonon frequencies are converged to within a few percent, which is small enough with respect to the intrinsic DFT error in LDA and GGA.

Calcium is a notoriously difficult element to pseudize. We perform a preliminary test for the GGA pseudopotential on CaO, another ionic compound of calcium, and find the relaxed lattice constants are within 1.6% of experiment. This precision is typical of GGA-DFT calculations. Fluorine is also a difficult element, but does not present a slower convergence in the full CaF_2 system.

To tackle dielectric properties, a more precise calculation is needed which includes the semicore (SC) $3s$ and $3p$ states for Ca: in this case a Hartwigsen-Goedecker-Hutter (HGH) (Ref. 23) pseudopotential is used with an energy cutoff of 100 Ha. The TM pseudopotentials present the advantage of having a low cutoff and being easily obtained in both the LDA and GGA. Adding semicore electrons to the TM potentials is possible but can be very involved, can generate ghost states, and can no longer present any advantage in terms of cutoff energies. HGH pseudopotentials are available only in the LDA, and present much higher cutoff energies. However, as they are cast directly as projectors and fitted, instead of being obtained by a Kleinman-Bylander (KB) (Ref. 24) transformation, they are not subject to the ghost states introduced by the KB procedure (see Ref. 25), and can be generated as easily for configurations with semicore electrons.

The Brillouin zone is sampled with an $8\times8\times8$ Monkhorst-Pack-type grid[26] (60 irreducible k points) with which the lattice constant is converged to within 10^{-5} Å.

The vibrational properties of CaF_2 are determined in linear response (perturbation theory), Refs. 27–30.

III. RESULTS

The experimental lattice parameter of CaF_2 is 5.4630 Å (Ref. 16) and in the GGA approximation we find 5.5637 Å with a 50 Ha plane-wave cutoff. The lattice parameter of CaF_2 is thus reproduced to within 2%, a normal agreement by GGA standards. The LDA pseudopotential gives a lattice parameter of 5.3519 Å, and underestimates a by 2%, which is also typical of the LDA. These results are of the same precision as those in Ref. 10, though their GGA [Perdew-Wang 1991] (Ref. 31) seems slightly better, i.e., to 1% of a.

A. Electronic properties

The band structure and density of states (DOS) for CaF_2 is represented in Fig. 1. The tetrahedron method[32,33] is used to generate an accurate DOS from 28 k points in the irreducible Brillouin zone. The zero in energy is set at the top of the valence band. The calculated indirect gap ($X\rightarrow\Gamma$) is seen to be 7.07 eV. Experimentally, the direct band gap is 12.1 eV and the indirect gap is estimated to be 11.8 eV.[34] It is well known that the local-density and generalized-gradient approximations to DFT systematically underestimate the band gap in semiconductors: the error of a factor of 2 is typical.

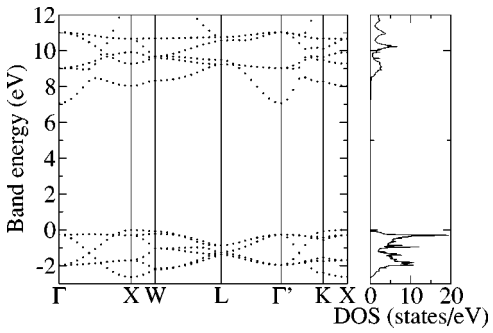

FIG. 1. Electronic band structure and DOS of CaF_2. The insulating gap of 7.1 eV is underestimated with respect to experiment (11.8 eV) as expected in a GGA-DFT calculation.

Our results agree well with the self-consistent field (SCF) results of Refs. 6 and 7, in particular, with those of Heaton and Lin,[7] who use a basis set of linear combinations of atomic orbitals, and a SCF method.

B. Electronic charge-density analysis

We carry out an analysis of the electronic density, using the Bader[35,36] and Hirshfeld[37] methods. We expect a clear ionic character in the bonding of CaF_2. These techniques allow us to quantify the ionicity, and to compare the different pseudopotentials. We will consider the experimental lattice parameter, giving a unit cell volume of 40.76 Å,[3] except where another a is specified.

The Bader method finds critical points of the Laplacian of the electronic density, and "bond paths" between atoms along which the density is maximal: in all directions perpendicular to the path, the density decreases. Along the path, the density is maximal at the atoms at both ends. The point along the path where the density is at a minimum defines a critical point. Further, a critical surface is defined: points of minimal density along different paths between atoms. This surface has zero flux of the density gradient through it. In this way the unit cell is cut up into basins of charge attributed to different atoms. Each basin has a certain volume, shape, and attributes the charge that it contains to its central atom.

We first consider the different pseudopotentials used. For each, the electronic density is generated and analyzed. The values of the Bader charges are presented in Table I. The

TABLE I. Atomic charges and volumes [in Å Ref. 3)] calculated by the Bader method, with different pseudopotentials and with a larger lattice parameter a. The changes vary a little with the pseudopotential or the value of a.

	SC-LDA	LDA	GGA	GGA 5.56 Å
Ca charge	1.647	1.648	1.665	1.679
Ca volume	11.61	11.40	11.40	11.94
F charge	−0.821	−0.824	−0.832	−0.838
F volume	14.85	14.58	14.58	15.39

difference between the two LDA pseudopotentials (with and without semicore electrons) is negligible: 0.001 electron on the calcium atom and 0.03 Å.[3] The difference with GGA is also small: 0.018 electrons and 0.03 Å.[3] We see that the bond is strongly ionic, as expected, but that the charge transfer is not complete. The volume of F is slightly larger, which could be due to the extra electron on F, or due to the differing geometry of the positions of F and Ca (the latter being of higher symmetry and with more neighbors).

Since we will consider two different lattice parameters for the phonons, we consider briefly the effect a has on the charges. Relaxing the structure with the GGA potential gives a lattice parameter of 5.56 Å. The last column in Table I contains the charges obtained in this case. The difference is minimal: 0.014 electrons with respect to the GGA case for the experimental value of a.

With the Bader analysis, we see the attributed charge is almost independent of the pseudopotential and lattice parameter used. The differences are slight between LDA and GGA, as is the variation of the charges with the cell volume. As the method depends mainly on the bonding region between the atoms, this comforts our assessment of the TM potentials as giving a good description of the bonding and chemistry of CaF_2, with a much smaller kinetic-energy cutoff.

The Hirshfeld method has been the subject of renewed interest in the quantum chemistry community over the past few years following the demonstration that it is a partitioning with maximal information.[38] The approach is somewhat different: first the total electronic densities of the isolated atoms or ''proatoms,'' are superposed in space. Then, the contribution of a proatom of type κ to the superposed density at a given point determines which fraction of the total electronic density will be attributed to κ. In this way, one obtains effective charge densities for each atom, the sum of which gives the total density. The densities can be integrated to give the apparent charge of the atom. The method was developed for atoms in molecules, where each atom is unique. In a solid-state context with periodic boundary conditions, we consider the sum of the proatomic densities from κ and all its translated images.

The Hirshfeld method gives small net charges on atoms. This follows many results obtained in the literature,[37,39,40] which suggest that the Hirshfeld charge transfer is systematically much smaller than the Bader one.

Using the GGA pseudopotential and the experimental lattice parameter, $Q_{Ca}=0.2377$ and $Q_F=-0.1188$. In LDA, the charges are $Q_{Ca}=0.1943$ and $Q_F=-0.0971$. The pseudopotential with semicore electrons gives $Q_{Ca}=0.3818$ and $Q_F=-0.1909$ electrons.

To test the effect of the lattice parameter, we calculate the charges in GGA with a slightly different value of the lattice parameter (5.49 Å), and obtain $Q_{Ca}=0.2731$ and $Q_F=-0.1366$.

We see that the Hirshfeld analysis is much more sensitive to the details of the calculation than the Bader analysis. The exchange-correlation potential can change the Hirshfeld charges significantly, although the order of magnitude and the direction of the transfer is the same. Since the proatom densities used in the different calculations are the same (for the GGA case both a GGA and a LDA proatom were tested and no difference was observed), the variation must come from the distribution of the electronic density between the atoms.

C. Dielectric properties

We describe and define here briefly the different dielectric properties we will consider. See Ref. 30 for the implementation and for the explanations of the notations used in this section. The electronic contribution to the dielectric constant, ϵ_∞ can be calculated from

$$\epsilon^{\infty}_{\alpha\beta}=\delta_{\alpha\beta}-\frac{4\pi}{\Omega_0}2E_{el}^{\mathcal{E}_\alpha\mathcal{E}_\beta}, \tag{1}$$

where $E_{el}^{\mathcal{E}_\alpha\mathcal{E}_\beta}$ is the second derivative of the total electronic energy with respect to a perturbing electric field along directions α and β, and Ω_0 is the unit cell volume. ϵ_∞ is typically measured in the visible spectrum for frequencies much smaller than the gap energy.

The variation of the force on a given atom, under the application of an electric field, defines the Born effective charge

$$Z^*_{\kappa,\alpha\beta}=\frac{\partial\mathcal{F}_{\kappa,\alpha}}{\partial\mathcal{E}_\beta}. \tag{2}$$

The additional contribution of phonons to the dielectric constant becomes important as $\omega\rightarrow 0$

$$\epsilon_{\alpha\beta}(\omega)=\epsilon^{\infty}_{\alpha\beta}+\frac{4\pi}{\Omega_0}\sum_{\kappa\kappa'}\sum_{\alpha'\beta'}Z^*_{\kappa,\alpha\alpha'}[\tilde{C}(\mathbf{q}=0) -\mathrm{M}\omega^2]^{-1}_{\kappa\alpha',\kappa'\beta'}Z^*_{\kappa',\beta\beta'}. \tag{3}$$

where M is the mass of the unit cell and $\tilde{C}$ is the Fourier transform of the matrix of interatomic force constants.

For dielectrics, there exists a sum rule for the second derivatives of the total energy with respect to atomic positions [the acoustic sum rule (ASR)—see Ref. 30]

$$\sum_{\kappa'}\frac{\partial E}{\partial R_{\kappa'\alpha'}\partial R_{\kappa\alpha}}=0. \tag{4}$$

The sum rule reflects the invariance of the forces on the atoms under uniform translation of all the atoms. The ASR is broken in our calculation, because of the representation of the XC potential on a discrete grid in real space: an infinitesimal displacement of the atoms will always change the XC grid.

The experimental and theoretical values of ϵ_∞, Z^*, and ϵ_0 are presented in Table II. Because of the cubic symmetry, the dielectric matrices and the Born effective charges for a given atom are all diagonal and have the same value along x,y, and z.

Globally, the HGH pseudopotential with SC electrons gives the best agreement with experiment. In most DFT dielectric constant calculations, ϵ_0 and ϵ_∞ are overestimated, and this is the case with the HGH pseudopotential. In our

TABLE II. Comparison of experimental dielectric constants and Born effective charges with those obtained in DFPT, using Troullier-Martins (LDA and GGA) and Hartwigsen-Goedecker-Hutter (LDA with semicore electrons) pseudopotentials. Two slightly different lattice parameters are considered: the experimental value 5.46 Å and a slightly larger 5.49 Å. Experimental data are taken from or cited in Ref. 3.

	a (Å)	ϵ_∞	$Z^*_{Ca,1,1}$	$Z^*_{F,1,1}$	ϵ_0
Experiment	5.46	2.28	+II	−I	6.76
LDA	5.46	2.06	+2.18	−1.09	5.30
LDA	5.49	2.05	+2.18	−1.09	5.57
GGA	5.46	2.03	+2.18	−1.09	4.92
GGA	5.49	2.02	+2.18	−1.09	5.14
LDA SC	5.46	2.32	+2.36	−1.18	9.02

calculations using the TM pseudopotentials, however, both dielectric constants are underestimated. We attribute this to the absence of core electrons in the calculation: though most of the phonon modes are well reproduced, the electronic response of the system remains incorrect. More specifically, the calcium atom has lost all of its valence electrons, and its core electrons should be dynamically rearranging themselves as a function of the phonon modes, which is naturally impossible in the frozen-core approximation.

The Born effective charges are close to the formal +II and −I charges for Ca and F in all cases. The calculated charges support our explanation of the differences between the phonon modes and dielectric constants with the different pseudopotentials: the charge for Ca is even higher when core electrons are free to move, with the HGH pseudopotential. The Born charges are larger than the Bader charges calculated in the preceding section, and vary more when semicore electrons are included. This is a further indication that, even if the ground-state density is correct, response function calculations are more sensitive to core electron effects and to the differences between pseudopotentials. Another part of the differences can be explained by the static or dynamic characteristics of the charges, as in Ref. 41.

The two Troullier-Martins pseudopotentials allow us to determine the effect of the exchange-correlation potential: there are no major differences in ϵ_∞ and the Z^*. On the other hand, ϵ_0 is higher in LDA than in GGA. This is due to the difference in the phonon eigenfrequencies, shown in the following section. The fact that LDA gives better results here is probably coincidental.

D. Vibrational properties

The phonon band structures in GGA and LDA, and the corresponding DOS are presented in Fig. 2. Eight irreducible q points are used for the interpolation of the interatomic force constants (IFC) in the Brillouin zone. The experimental data of Elcombe and Pryor[3] are included as circles. Both GGA and LDA give good band structures, and the LDA values are closer to experiment than GGA. For the acoustic branches, the agreement is excellent.

Phonon frequencies at Γ are presented in Table III. As can

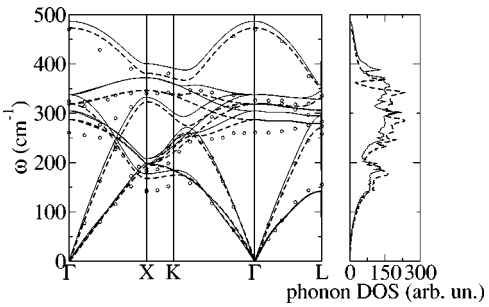

FIG. 2. (Left) Phonon band structure of CaF_2 using Troullier-Martins pseudopotentials for $a=5.49$ Å. Frequencies in cm^{-1}: continuous line = GGA, dashed line = LDA. The circles are experimental data from Ref. 3. (Right) Phonon density of states in GGA (continuous line) and LDA (dashed line).

be seen in Fig. 2, the main disagreement occurs at Γ for the first optical mode. Compared to the values of Refs. 43, 45, and for the experimental lattice constant, the difference is ~12% in LDA and 18% in GGA. Between K and X there is also a difference on the same order, for the analogous phonon branch (the first optical mode). In general, for optical branches, a 10% error in LDA or GGA can be considered acceptable, although much better results are obtained for simple, covalently bonded systems.[27,28] The zone-center frozen-phonon calculations in Ref. 10 give more homogeneous accuracy: better values for the infrared-(IR) active mode but worse for the Raman mode (errors of ~7 to 8% in LDA and GGA). The authors do not specify whether the experimental or the relaxed lattice parameter is used (see below).

The sizable difference in frequencies for the first optical mode calls for an explanation; we examine two main factors: the lattice parameter and the pseudopotential.

In some systems the phonon frequencies can be very sensitive to the lattice parameter a. Values are shown for the experimental lattice constant 5.46 Å, as well as for a slightly different value of 5.49 Å. A shift is observed, of between 8 and 15 cm^{-1}, i.e., up to 6%. However, the improvement when using the experimental lattice constant is not systematic: for LDA the results are generally worse and for GGA better. This implies that the larger lattice parameter compensates the LDA error on the frequencies and aggravates the GGA error.

The other main source of discrepancy is the pseudopotential used: the Troullier-Martins potentials are fairly soft, as semicore electrons are not treated explicitly, but are frozen into the ionic core. A nonlinear-core correction is used to include the response of the outer core electrons and works well for ground-state properties (in particular, the lattice constants). However, the transverse optical phonon frequencies at Γ depend on the electronic response to the polarization induced by the phonon [which gives the splitting between the longitudinal and transverse optical modes (LO-TO)]. Here the NLCC correction seems insufficient.

In order to quantify the effect of the different pseudopotential approximations, we employ a more accurate HGH pseudopotential for Ca, with $3s$ and $3p$ semicore electrons. Our first observation is that the convergence with this

TABLE III. Comparison of experimental Γ point frequencies (cm^{-1}) with those obtained in DFPT, using Troullier-Martins (LDA and GGA) and Hartwigsen-Goedecker-Hutter (LDA-SC) pseudopotential for Ca. Imposing the acoustic sum rule changes the optical phonon frequencies significantly in the HGH case. For the pseudopotentials without SC the effect is very small; the results are shown after imposition of the ASR.

	a (Å)	T_{1u}-TO (IR)	Diff	T_{2g} (Raman)	Diff	T_{1u}-LO	Diff
Experiment	5.46	257.2 [a], 270 [b]		322.2 [c], 327.5 [d]		466.4 [a]	
LDA	5.46	301.7	(17.3%,11.7%)	328.9	(2.1%,0.5%)	484.3	(3.8%)
LDA	5.49	287.0	(11.6%,6.3%)	318.7	(1.1%,2.7%)	473.1	(1.4%)
GGA	5.46	319.5	(24.2%,18.3%)	347.8	(8.0%,6.2%)	497.8	(6.8%)
GGA	5.49	304.9	(18.6%,13.0%)	337.6	(4.8%,3.1%)	486.5	(4.4%)
LDA SC	5.46	227.1	(11.7%,15.9%)	298.9	(7.2%,8.7%)	447.8	(4.0%)

[a]Reference 42.
[b]Reference 43.
[c]Reference 44.
[d]Reference 45.

pseudopotential is much more difficult. With a plane-wave kinetic-energy cutoff of 100 Ha the total energy and forces are converged. Our results for the HGH pseudopotentials (with SC) are included in Table III. The improvement for the phonon frequencies over the TM pseudopotential is not systematic, but as shown above the dielectric properties change dramatically. The HGH calcium pseudopotential underestimates the modes, whereas the TM overestimates them.

The anharmonicity of the phonon modes would necessitate higher-order perturbations to be reproduced, but is probably not a problem in our case. Strock and Batterman[46] studied the anharmonicity of CaF_2's vibrational modes as a function of temperature and showed that the effect remains small at low temperatures ($\leqslant$300 K).

E. Interatomic force constants

Finally, we analyze the behavior of the interatomic force constants in real space. $\Phi_{ij}^{a\kappa,a'\kappa'}$ denotes the IFC exerted on atom κ' in cell a' in direction j, when atom κ in cell a undergoes a unit displacement along i. $\Phi_{ij}^{a\kappa,a'\kappa'}$ is the Fourier transform of the dynamical matrix, obtained from the second variation of the total energy with respect to atomic positions. The IFC can be decomposed into an electrostatic (Ewald) contribution, which is long ranged, and a ''local'' contribution which can be attributed to covalent bonding. The behavior of the total IFC and of the local contribution, as a function of interneighbor distance, is shown in Fig. 3. The top figure shows the longitudinal IFC for calcium-calcium interactions, the middle one for calcium-fluorine, and the lower one for fluorine-fluorine interactions. In each case the total IFC decays as $1/r^3$ for large r, as shown by the fitting curve.

For each species pair, we consider the extent of the local part of the IFC to characterize the interaction. For the Ca-F interaction, the local part goes to zero very quickly—it is reduced to less than 6% of the total after the nearest Ca-F neighboring pair (after 4.6 Å). For Ca-Ca and F-F, however, the local part stays large and changes sign several times before decaying. Only at the third Ca-Ca neighbor does

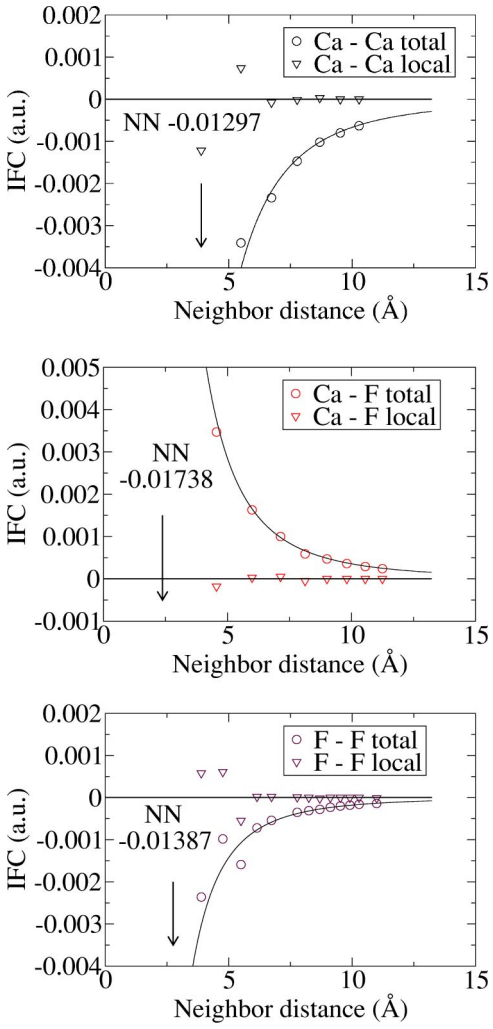

FIG. 3. Longitudinal projection of the interatomic force constants between (upper) Ca and Ca atoms, (middle) Ca and F atoms, (lower) F and F atoms. The IFC are decomposed into a local and a Ewald (electrostatic) component. The latter is fitted by a $1/r^3$ function, and the local part vanishes quickly. The position and value of the nearest-neighbor IFC is shown with an arrow.

$\Phi^{Ca,Ca}_{local}/\Phi^{Ca,Ca}_{total}$ become less than 3% (6.73 Å). The F-F interaction becomes small ($<3\%$) only for the fifth F-F neighbor (6.14 Å). The knowledge of the IFC is the basis for understanding the deformations induced by line or point defects, such as impurities or vacancies. The fact that differing Ca F ions are almost independent after a very short distance is striking given the extent of the same-species interactions. A point defect, for example, will interact mainly with same-species sites to distances up to 6 or 7 Å. This gives an estimation of the supercell size needed to correctly calculate defect properties in fluorite.

Our database of dynamical matrices and the IFC analysis for CaF_2 is available on the world wide web at ftp://ftp.mapr.ucl.ac.be/pub/outgoing/MVERSTRA/

IV. CONCLUSION

The electronic structure, dielectric properties, and vibrational properties of calcium difluoride are presented, determined using density-functional theory. The electronic properties of CaF_2 are well reproduced in our calculations, apart from the usual DFT band-gap underestimation. We compare atomic charges calculated by the Bader and Hirshfeld methods. The Bader charges are insensitive to changes in the pseudopotentials or in the lattice parameters, which implies that the bonding and chemistry does not depend too strongly on the presence of semicore electrons. The Hirshfeld charges, however, vary much more strongly, which demonstrates that a real variation of the local charge density around the atoms does occur when one switches from one pseudopotential to another. The equilibrium lattice parameter is well reproduced with all the different pseudopotentials. The phonon band structures are much more delicate. Those obtained using both the LDA and GGA pseudopotentials have the correct shape, and reproduce most of the phonon branches correctly, except the lowest T_{1u} branch around Γ and from X to K. This is accompanied by an underestimation of the dielectric constants and, to a lesser extent, of the Born effective charges. We show that the error stems from the frozen-core approximation and that by including semicore $3s$ and $3p$ states (with a LDA-HGH pseudopotential) this can be remedied. However, the HGH potential has its own drawbacks, including a very high cutoff energy. The interatomic force constants are analyzed and separated into local and electrostatic contributions. The distance at which the local part decays (7 Å for the F-F and Ca-Ca IFC) determines the size of the supercell needed to simulate defects which are isolated.

ACKNOWLEDGMENTS

Part of this research has been supported by the FRFC Project No. 2.4556.99, the Action de Recherche Concertée ''Interaction électron-vibration dans les nanostructures,'' and the Research Training Network contract No. HPRN-CT-2002-00317 ''First−principles approach to the calculation of the optical properties of Solids.'' X.G. acknowledges financial support from the FNRS. We wish to thank P. Casek and F. Finocchi for the implementation of the Bader atom-in-molecule method.

*Electronic address: verstraete@pcpm.ucl.ac.be

[1] J.H. Burnett, Z.H. Levine, and E.L. Shirley, Phys. Rev. B **64**, 241102 (2001).
[2] D.M. Boye, R.M. Macfarlane, Y. Sun, and R.S. Meltzer, Phys. Rev. B **54**, 6263 (1996).
[3] M.M. Elcombe and A.W. Pryor, J. Phys. C **3**, 492 (1970).
[4] A.K. McCurdy, Phys. Rev. B **26**, 6971 (1982).
[5] A. Feldman and R.M. Waxler, Phys. Rev. Lett. **45**, 126 (1980).
[6] J.P. Albert, C. Jouanin, and C. Gout, Phys. Rev. B **16**, 4619 (1977).
[7] R.A. Heaton and C.C. Lin, Phys. Rev. B **22**, 3629 (1980).
[8] L.X. Benedict and E.L. Shirley, Phys. Rev. B **59**, 5441 (1999).
[9] N.H. de Leeuw, J.A. Purton, S.C. Parker, G.W. Watson, and G. Kresse, Surf. Sci. **452**, 9 (2000).
[10] M. Mérawa, M. Llunell, R. Orlando, M. Gelize-Duvignau, and R. Dovesi, Chem. Phys. Lett. **368**, 7 (2003).
[11] K. Schmalzl (unpublished).
[12] P. Hohenberg and W. Kohn, Phys. Rev. **136**, 864 (1964).
[13] W. Kohn and L.J. Sham, Phys. Rev. **140**, A1133 (1965).
[14] X. Gonze, J.-M. Beuken, R. Caracas, F. Detraux, M. Fuchs, G.-M. Rignanese, L. Sindic, M. Verstraete, G. Zerah, F. Jollet, M. Torrent, A. Roy, M. Mikami, Ph. Ghosez, J.-Y. Raty, and D.C. Allan, Comput. Mater. Sci. **25**, 478 (2002). Note: ABINIT is a common project of the Université Catholique de Louvain, Corning Incorporated, and other contributors (http://www.pcpm.ucl.ac.be/ABINIT).
[15] M.C. Payne, M.P. Teter, D.C. Allan, T.A. Arias, and J.D. Joannopoulos, Rev. Mod. Phys. **64**, 1045 (1992).
[16] R. W. G. Wyckoff, *Crystal Structures*, 9th ed. (Interscience/John Wiley, New York, 1963), vol. 1.
[17] C.G. Broyden, Math. Comput. **19**, 577 (1965).
[18] J.P. Perdew and Y. Wang, Phys. Rev. B **45**, 13 244 (1992).
[19] D.M. Ceperley and B.J. Alder, Phys. Rev. Lett. **45**, 566 (1980).
[20] J.P. Perdew, K. Burke, and M. Ernzerhof, Phys. Rev. Lett. **77**, 3865 (1996).
[21] N. Troullier and J.L. Martins, Phys. Rev. B **43**, 1993 (1991).
[22] S.G. Louie, S. Froyen, and M.L. Cohen, Phys. Rev. B **26**, 1738 (1982).
[23] C. Hartwigsen, S. Goedecker, and J. Hutter, Phys. Rev. B **58**, 3641 (1998).
[24] L. Kleinman and D.M. Bylander, Phys. Rev. Lett. **48**, 1425 (1982).
[25] X. Gonze, P. Käckell, and M. Scheffler, Phys. Rev. B **41**, 12 264 (1990).
[26] H.J. Monkhorst and J.D. Pack, Phys. Rev. B **13**, 5188 (1976).
[27] S. Baroni, S. de Gironcoli, A. Dal Corso, and P. Giannozzi, Rev. Mod. Phys. **73**, 515 (2001).
[28] P. Giannozzi, S. de Gironcoli, P. Pavone, and S. Baroni, Phys. Rev. B **43**, 7231 (1991).
[29] X. Gonze, Phys. Rev. B **55**, 10337 (1997).
[30] X. Gonze and C. Lee, Phys. Rev. B **55**, 10355 (1997).
[31] J. P. Perdew and Y. Wang (unpublished).
[32] G. Lehmann and M. Taut, Phys. Status Solidi B **54**, 469 (1972).
[33] P.E. Blöchl, O. Jepsen, and O.K. Andersen, Phys. Rev. B **49**, 16223 (1994).

[34] G.W. Rubloff, Phys. Rev. B **5**, 662 (1972).
[35] R.F.W. Bader, MTP Int. Rev. Sci.: Phys. Chem. Ser. Two **1**, 43 (1975).
[36] R.F.W. Bader, J. Phys. Chem. **102**, 7314 (1998).
[37] F.L. Hirshfeld, Theor. Chim. Acta **44**, 129 (1977).
[38] R.F. Nalewajski and R.G. Parr, J. Phys. Chem. A **105**, 7391 (2001).
[39] J. Meister and W.H.E. Schwarz, J. Phys. Chem. **98**, 8245 (1994).
[40] K.B. Wiberg and P.R. Rablen, J. Comput. Chem. **14**, 1504 (12) (1993).
[41] P. Ghosez, J.-P. Michenaud, and X. Gonze, Phys. Rev. B **58**, 6224 (1998).
[42] W. Kaiser, W.G. Spitzer, R.H. Kaiser, and L.E. Howarth, Phys. Rev. **127**, 1950 (1962).
[43] R.P. Lowndes, J. Phys. C **3**, 3083 (1971).
[44] J.P. Russel, Proc. Phys. Soc. London **85**, 194 (1965).
[45] P. Denham, G.R. Field, P.L.R. Morse, and G.R. Wilkinson, Proc. R. Soc. London, Ser. A **317**, 55 (1970).
[46] H.B. Strock and B.W. Batterman, Phys. Rev. B **5**, 2337 (1972).